ISSN 1028-3358, Doklady Physics, 2015, Vol. 60, No. 5, pp. 217–223. © Pleiades Publishing, Ltd., 2015.
Original Russian Text © L.G. Kurakin, I.V. Ostrovskaya, M.A. Sokolovskiy, 2015, published in Doklady Akademii Nauk, 2015, Vol. 462, No. 2, pp. 161–167.

MECHANICS

Stability of Discrete Vortex Multipoles in Homogeneous and Two-Layer Rotating Fluid

L. G. Kurakin[a, b], I. V. Ostrovskaya[a], and M. A. Sokolovskiy[c, d]*

Presented by Academician R.I. Nigmatulin September 17, 2014

Received September 22, 2014

DOI: 10.1134/S1028335815050067

The problem of stability of multipolar vortex structures has been investigated intensively since the works by Kelvin, Gröbli Goryacheva, and Joukowski [1, 2]. The deepest advance in its solution took place within the framework of the model of point vortices on a plane (the Kirchhoff equations). The efforts of many authors were accomplished in [3] in the form of a mathematically rigorous solution of the Kelvin problem of stationary rotation stability of a set of identical point vortices located on a plane at vertices of a regular N-gon. For this purpose, the concept of generalized steady motions of dynamic systems with symmetry was introduced, and a special approach to the problem of their stability in the Routh sense was developed. On its basis, it was proved that the maximum number of point vortices located at the verices of a stable regular vortex polygon is seven. The approach developed in [3] was applied to the solution of the Kelvin problem for vortices on a sphere [4], in a ring [7], and inside and outside a circle [5, 6].

Numerous investigations [1, 2] have been devoted to the discrete vortex structure of the $N + 1$ type (an equilateral vortex N-gon with a central vortex of arbitrary intensity). The linear analysis of its stability is given in [8] for the Kirchhoff equations with an arbitrary N and in [9] for a geostrophic 2D single-layered model in the approximation of the f plane and $N \le 10$.

In this study, we consider a two-layer quasi-geostrophic model in the approximation of the f plane [2]. The methods of [3] are used for analyzing the stability of the discrete vortex structure of the $N + 1$ type ($N = 2, 3$). It is confirmed by numerical calculation of vortex trajectories. We also investigated the limiting case of a homogeneous fluid. The particular results of this problem were obtained in [10, 11] (see remark 1).

FORMULATION OF THE PROBLEM

We consider a set of $N + 1$ point vortices in a two-layer fluid. Let $v_k = (x_k, y_k)$ be the Cartesian coordinates of the kth vortex ($k = 0, 1, ..., N$). The vortices $v_1, ..., v_N$ are located in one layer (for definiteness, in the lower layer), and they have an identical intensity κ. The vortex v_0 has the intensity κ_0. Further, we distinguish the following cases:

(I) the vortex v_0 is in the upper layer with a thickness h_1;

(II) all $N + 1$ vortices are located in the lower layer with a thickness h_2.

Let $h_1 + h_2 = 1$, and the effective intensities be: $\kappa h_2 = 1$ for identical vortices and $\kappa_0 h_1 = \Gamma$ for the vortex v_0 in the case (I) or $\kappa_0 h_2 = \Gamma$ in the case (II). We introduce the designations for the generalized coordinates $q_j = x_j$ ($j = 0, 1, ..., N$) and for the generalized momenta $p_0 = \Gamma y_0$, $p_k = y_k$ ($k = 1, 2, ..., N$).

The motion of the vortex system under consideration is described by the Hamiltonian $\mathcal{H}(q, p)$, $q = (q_0, ..., q_N)$, $p = (p_0, ..., p_N)$ [12]:

$$\mathcal{H} = -\frac{1}{4\pi}\left[\Gamma\sum_{k=1}^{N} V\left(\sqrt{(q_0 - q_k)^2 + \left(\frac{p_0}{\Gamma} - p_k\right)^2}\right) + \sum_{1 \le j < k \le N} W\left(\sqrt{(q_j - q_k)^2 + (p_j - p_k)^2}\right)\right]. \quad (1)$$

[a] Southern Federal University, Rostov-on-Don, 344049 Russia
[b] Southern Mathematical Institute, Vladikavkaz Science Center, Russian Academy of Sciences, Vladikavkaz, Northern Osetiya, 362040 Russia
[c] Water Problems Institute, Russian Academy of Sciences, Moscow, 107078 Russia
[d] Shirshov Institute of Oceanology, Russian Academy of Sciences, Moscow, 117997 Russia
*e-mail: sokol@aqua.laser.ru

The functions V and W have the form

$$W(\xi) = \ln\xi - \frac{1-\alpha}{1+\alpha}K_0(\gamma\xi),$$

$$V(\xi) = \begin{cases} \ln\xi + K_0(\gamma\xi) & \text{in case I,} \\ W(\xi) & \text{in case II.} \end{cases}$$

Here, K_0 is the modified Bessel function, $\frac{1}{\gamma} > 0$ is the internal Rossby radius of deformation [2], $\alpha = \frac{h_2 - h_1}{2}$, so $h_1 = \frac{1-\alpha}{2}$, $h_2 = \frac{1+\alpha}{2}$, and the condition $-1 < \alpha < 1$ is fulfilled.

The system with the Hamiltonian (1) has four integrals: the energy $\mathcal{H}(q, p)$, the linear momentum components I_1 and I_2, and the total angular momentum M:

$$I_1 = \sum_{k=1}^{N} q_k + \Gamma q_0, \quad I_2 = \sum_{k=0}^{N} p_k,$$

$$M = \sum_{k=1}^{N} (q_k^2 + p_k^2) + \Gamma q_0^2 + \frac{p_0^2}{\Gamma}.$$

Passing to the variables $z_k = q_k + ip_k$ and $\bar{z}_k = q_k - ip_k$, we obtain

$$\dot{\bar{z}}_k = 2iH_k, \quad \dot{z}_k = -2iH_{z_k}, \quad k = 0, 1, \ldots, N. \quad (2)$$

Here, the Hamiltonian $H = \mathcal{H}(q(z, \bar{z}), p(z, \bar{z}))$ and the variable $z = (z_0, z_1, ..., z_N)$. The phase space Z of the system (2) is $\mathbb{C}^{N+1}$ with cuts along all hyperplanes $z_j = z_k$, $j \neq k$ ($j, k = 1, 2, ..., N$ in the case (I) and $j, k = 0, 1, ..., N$ in the case (II)).

The system (2) is invariant with respect to the group $\mathcal{G}$ of Euclidian motions of the plane $\mathbb{R}^2$. The action $g \mapsto L_g$ of this group on the phase space Z is determined by the equality $L_g z = (gz_0, gz_1, ..., gz_N)$ for any arbitrary point $z = (z_0, z_1, ..., z_N) \in Z$ and any arbitrary motion $g \in \mathcal{G}$. Thus, all points $z_0, z_1, ..., z_N$ are subject to the same transformation g. The generatrices of the group $\mathcal{G}$ are the mirror reflection j: $z \mapsto \bar{z}$, the translation g^{tr}: $z \mapsto z + \eta$, $\eta \in \mathbb{C}$, and the rotation g^{rot}: $z \mapsto e^{i\beta}z$, $\beta \in \mathbb{R}$. It should be noted that, according to Noether's theorem [13], the integrals I_1 and I_2 of the linear momentum arise as a consequence of the translational invariance of the Hamiltonian H, while the integral of the angular momentum M arises as a consequence of its invariance with respect to the rotation. We recall that the stationary motion is implemented by the transformation of a certain one-parametrical subgroup of the symmetry group of this equation (see, for example, [3]).

We find the stationary motion corresponding to the subgroup of rotations g^{rot} as $z_k = e^{i\omega t}u_k$, where unknowns $u_0, u_1, \ldots, u_N \in \mathbb{C}$, $\omega \in \mathbb{R}$. In the cases $N = 2, 3$, examples of such motion are the following solutions:

$$z_0(t) = 0, \quad z_j(t) = R\exp\left\{i\left(\frac{2\pi(j-1)}{N} + \omega_N t\right)\right\},$$
$$R > 0, \quad j = 1, 2, \ldots, N,$$
$$\omega_2 = \frac{1}{4\pi R}(\Gamma V'(R) + W'(2R)), \quad (3)$$
$$\omega_3 = \frac{1}{4\pi R}(\Gamma V'(R) + \sqrt{3}W'(\sqrt{3}R)),$$

in the form of the configuration of N identical vortices of the lower layer located uniformly on the circle of the radius R and rotating with a constant angular velocity $\omega_N(\Gamma, R)$ around the $(N+1)$-th vortex. In [10], solution (3) in the case (I) is called the "roundabout."

The replacement of variables $z_k(t) = e^{i\omega_N t}\zeta_k(t)$, $k = 0, 1, ..., N$ in the system (2) results in the equation of relative motion with the relative Hamiltonian (in the terminology of [3])

$$E(\zeta) = H(\zeta) + \frac{\omega_N}{2}M(\zeta),$$

$$\zeta = (\zeta_0, \zeta_1, \ldots, \zeta_N) \in \mathbb{C}^{N+1}.$$

On each plane of the variables ζ_j ($j = 1, 2, ..., N$), we introduce quasi-polar coordinates $\zeta_j = \sqrt{R^2 + 2r_j}\exp\left[i\left(\frac{2\pi(j-1)}{N} + \theta_j\right)\right]$. In the variables $\rho = (q_0, r_1, ..., r_N, p_0, \theta_1, ..., \theta_N)$, we obtain the equations of motion with the Hamiltonian $E(\zeta(\rho))$.

The continuous family of equilibria $\mathcal{C} = \{\rho \in \mathbb{R}^{2(N+1)} : q_0 = r_1 = \ldots = r_N = p_0 = 0, \theta_1 = \ldots = \theta_N\}$ corresponds to solution (3). *As the stability of solution* (3) *by Routh, we understand the stability of the family of equilibria* $\mathcal{C}$ *by Lyapunov* (see [3]). It should be noted that for proving such stability, it suffices to find a positive-term integral, which is positively defined with regard to the variables, in a subspace orthogonal to the family of equilibria $\mathcal{C}$.

Let $E_2 = (S\rho, \rho)$ be the square terms of the expansion of the Hamiltonian $E(\zeta(\rho))$ in the Taylor series with respect to the variable ρ in the vicinity of the zero equilibrium position, and let L be the corresponding linearization matrix. The matrix S is symmetric and has the zero eigenvalue corresponding to the family $\mathcal{C}$. The sufficient condition of stability by Routh for solution (3) means that all other eigenvalues of the matrix S have the same sign. The exponential instability takes

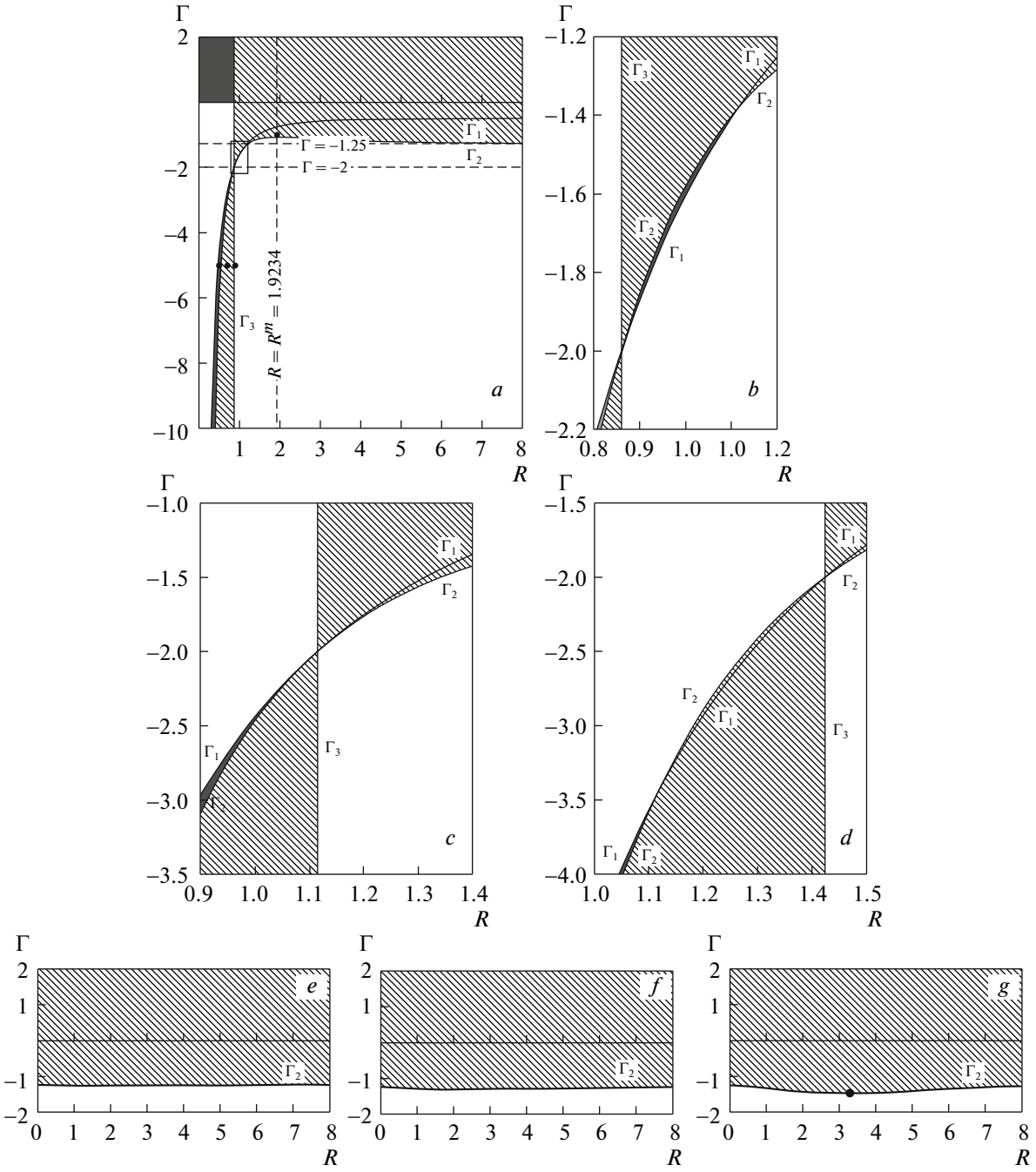

Fig. 1. Diagrams of stability of the tripole ($N = 2$): (*a*–*d*) the vortex roundabout (case I), (*e*–*g*) the vortices in one layer (case II).

place when the matrix L has eigenvalues with a positive real part.

FORMULATION OF THE RESULT

The analytical investigation of eigenvalues of the matrices S and L has shown that the half-plane of parameters (R, Γ), $R \geq 0$, is divided into regions of three types (see Figs. 1, 2).

A. The dark region is the stability by Routh in the nonlinear formulation. The eigenvalues of the matrix S, except for the simple zero, are positive.

B. The dashed region is the exponential instability.

C. White region. The eigenvalues of the matrix S have different signs, and they are all pure imaginary for the matrix L. In this case, the nonlinear analysis is necessary for the conclusion about stability.

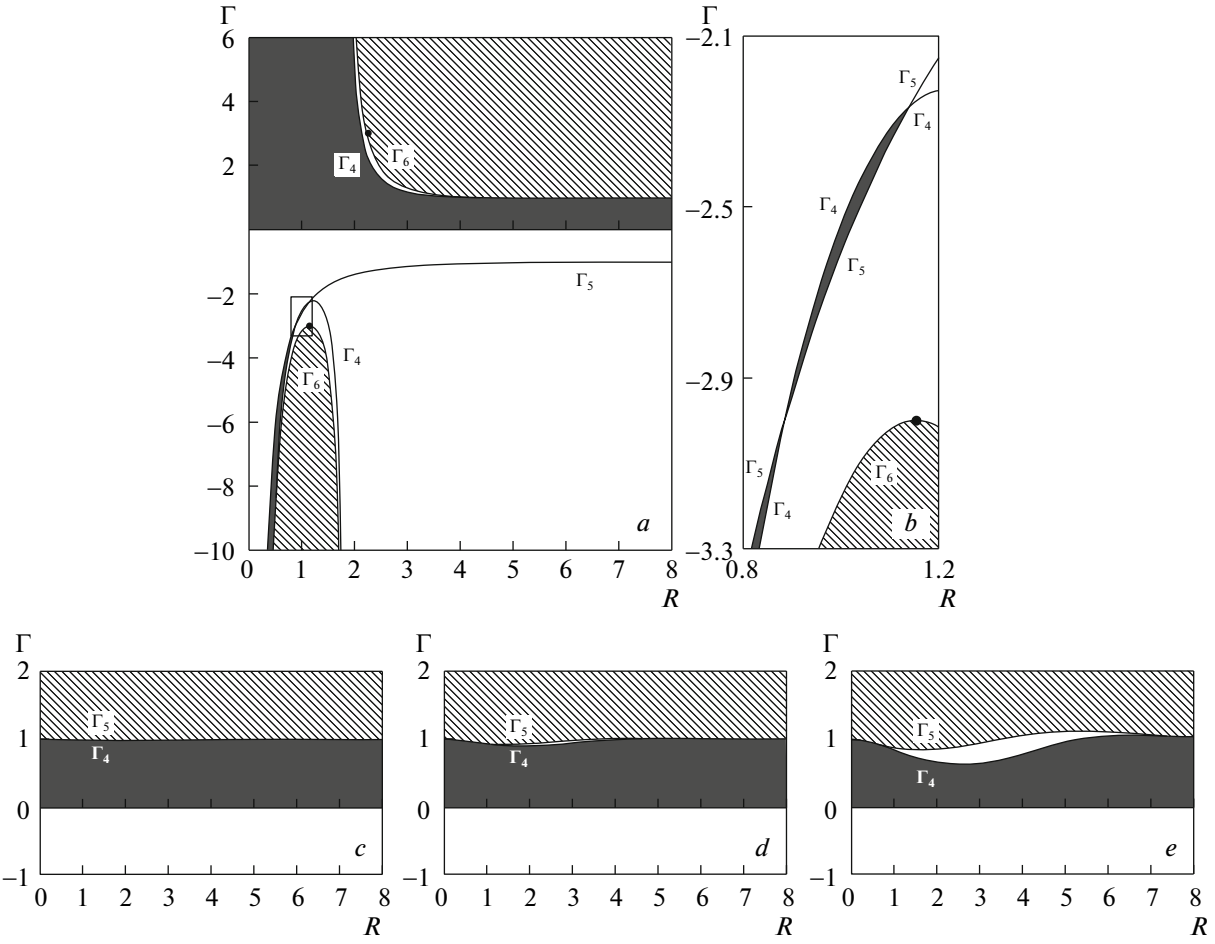

Fig. 2. The same as in Fig. 1 for quadrupole ($N = 3$).

The curves $\Gamma_j, j = 1, ..., 6$, in Figs. 1 and 2 are set by formulas

$$\Gamma_1(R) = -\frac{Y_1}{X_1}, \quad \Gamma_2(R) = \frac{2RX_2 - Y_1}{X_1 - RX_2},$$

$$\Gamma_3 = \{(\Gamma, R_*) \in \mathbb{R}^2 : R = R_*\},$$

$$\Gamma_4(R) = \frac{(2Z_1 - \sqrt{3}RX_2 - \sqrt{3}X_1)(Z_1 - \sqrt{3}RZ_2)}{(-X_1 + RX_2)(\sqrt{3}Z_1 - 2X_1 - RZ_2)},$$

$$\Gamma_5(R) = -\frac{\sqrt{3}Z_1}{X_1},$$

$$\Gamma_6(R) = -\frac{3(RX_2 + X_1 + RZ_2 - \sqrt{3}Z_1)^2}{4(X_1 - RX_2)(\sqrt{3}Z_1 - 2X_1 - RZ_2)}.$$

Here, we have introduced the following designations: $X_1 = V'(R)$, $X_2 = V''(R)$, $Y_1 = W'(2R)$, $Y_2 = W''(2R)$, $Z_1 = W'(\sqrt{3}R)$, $Z_2 = W''(\sqrt{3}R)$, and the value of R_* is the root of the equation $Y_1(R) - 2X_1(R) = 0$. The case $\gamma \neq 1$ reduces to the case $\gamma = 1$ by the scale replacement $R \mapsto R\gamma$.

The positions of the markers on panels *a* and *g* in Fig. 1 and panels *a* and *b* in Fig. 2 correspond to the initial states for the numerical experiments in Figs. 3 and 4, respectively. The results of the stability analysis for the vortex tripole ($N = 2$) are shown in Fig. 1 and those for the quadrupole ($N = 3$) are shown in Fig. 2.

Case I: Vortices in different layers. The positions *a* and *b* in Fig. 1 correspond to the case of identical thickness $h_1 = h_2 = \frac{1}{2}$ ($\alpha = 0$). In Fig. 1*b*, we show the intersection of curves Γ_1 and Γ_2 in the rectangular region singled out in Fig. 1*a* on a large scale. The positions in Figs. 1*b*–1*d* describe the change in the topological division of the space of parameters into three region types, when the decreasing parameter α passes through the critical values $\alpha_* = -0.5419$, namely, $\alpha = 0 > \alpha_*$ on the panel *b*, $\alpha = \alpha_*$ on the panel *c*, and $\alpha = -0.8 < \alpha_*$ on the panel *d*. The special case, when the

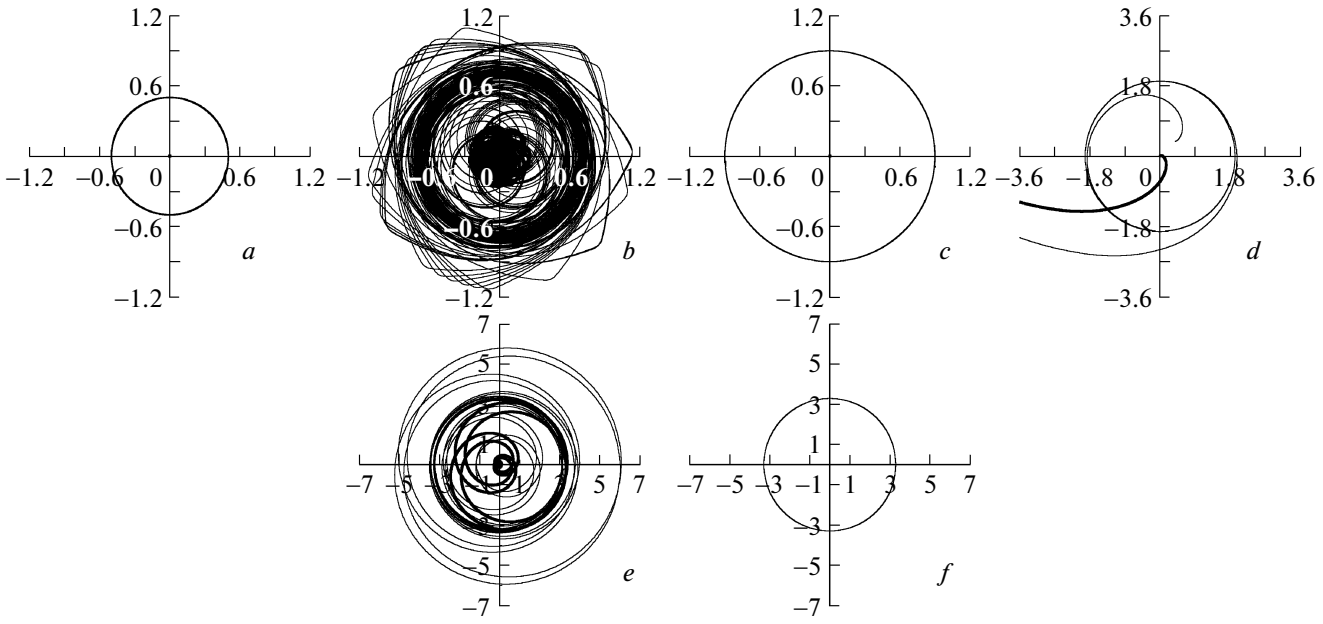

Fig. 3. Trajectories of the absolute motion of vortices in the tripolar roundabout (*a*–*d*) and of the tripolar vortex structure of the lower layer (*e*–*f*).

curves Γ_1 and Γ_2 touch each other, corresponds to the point $\alpha = \alpha_*$, and the pit-shaped region between the points of their intersection shrinks to one point. In the remaining part of the domain of parameters (R, Γ), the character of such a division depends only weakly on the parameter α, i.e., qualitatively the same as in Fig. 1*a*.

Figures 2*a* and 2*b* have the same meaning as in Figs. 1*a* and 1*b* but for the case of quadrupole roundabouts ($N = 3$). Here, $\alpha = 0.8$. The critical value of $\alpha_{**} = -0.6903$ plays the same role as α_* in the case $N = 2$.

Case II: Vortices in one layer. The vortex tripole structure of the lower layer ($N = 2$) is exponentially unstable, when $\Gamma > \Gamma_2$, and is linearly stable (nonlinear analysis is required) for $\Gamma < \Gamma_2$ (see Figs. 1*e*–1*g*).

In Figs. 2*c*–2*e*, we show the diagrams of stability for the quadrupole structures of the lower layer at $\alpha = 0.8$, $\alpha = 0$, and $\alpha = -0.8$, respectively. Here the region of exponential instability is located above the curve Γ_5, and the domain of stability by Routh is limited from above by the neutral curve Γ_4 and from below by the straight line $\Gamma = 0$. The investigation of stability in the regions $\Gamma_4 \le \Gamma \le \Gamma_5$ and $\Gamma < 0$ requires a nonlinear analysis.

In Figs. 3 and 4, we show the calculated trajectories of the vortices confirming the results of the stability analysis. For example, in Figs. 3*a*–3*d*, there are given the trajectories of the absolute motion of vortices of the tripolar roundabout at $N = 2$, $\alpha = 0$: on panels a–c $\Gamma = -5$ and $R = 0.5$, $R = 0.7$, and $R = 0.9$, respectively; and on the panel *d* $(R, \Gamma) = (R^m, -1)$. Here $R^m = 1.9234$, where the largest value of $\Gamma^m = \max\Gamma_2 = -1.0694$ is achieved. In Fig. 1*a*, the markers correspond to these experiments. In Figs. 3*e* and 3*f*, the trajectories of peripheral vortices (fine lines) and the central vortex (bold lines) of the tripolar vortex structure of the lower layer are shown at $\alpha = -0.8$: $(R, \Gamma) = (3.2894, -1.45)$ (*e*), $(R, \Gamma) = (3.2894, -1.50)$ (*f*). The markers corresponding to these experiments are almost indistinguishable in Fig. 1*g*: the first of them is located somewhat above curve Γ_2, and the second is a little lower. The fragments *b*, *d*, and *e* show the unstable state of the vortex structures. Figure 4 gives examples of trajectories of peripheral vortices (fine lines) and the central vortex (bold line) of the unstable quadrupolar roundabouts at $N = 3$, $\alpha = 0.8$. On panels *a* and *b*, $(R, \Gamma) = (1.1540, -3.0001)$. The markers in the domain of instability near its boundary at $\Gamma = \max|_{R<R_*}\Gamma_6 = -3$ in Figs. 2*a* and 2*b* correspond to this experiment. On panels *c* and *d*, $(R, \Gamma) = (2.2600, 3)$. The marker in the upper half-plane of Fig. 2*a* corresponds to this experiment. Here, Figs. 4*a* and 4*c* show the absolute motion of vortices; Figs. 4*b* and 4*d* show the motion of peripheral vortices with respect to the central vortex.

Remark 1. The numerical analysis of stability of the vortex roundabout for $N = 2$ and $\alpha = 0$ is carried out in [10]. In [11], the stability of the vortex roundabout for $N = 2$, 3, 4 and $\alpha = 0$ was investigated. The classical

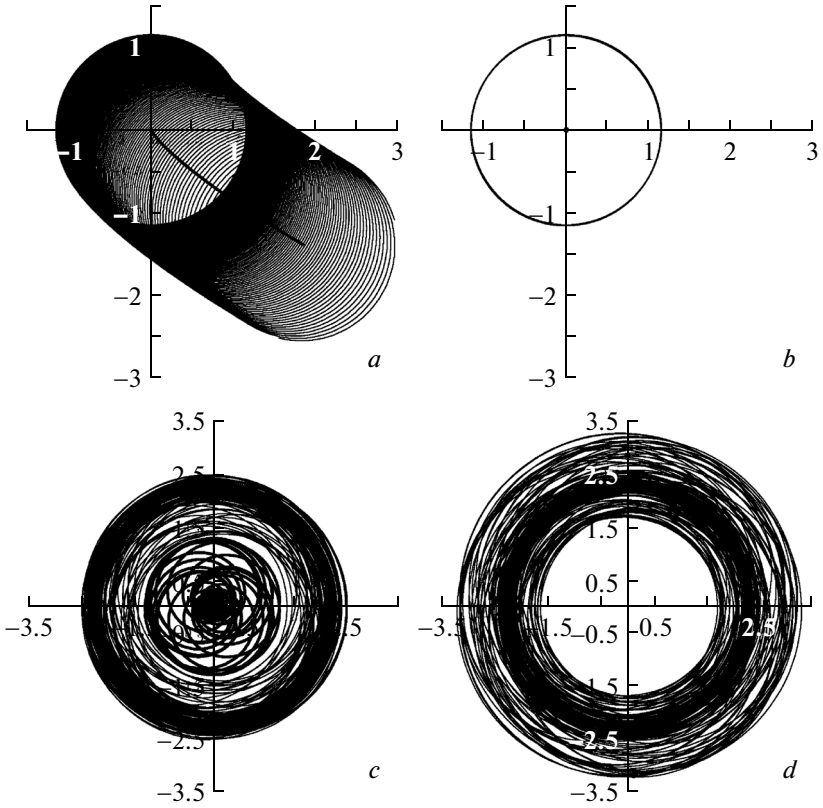

Fig. 4. Absolute (*a*, *c*) and relative (*b*, *d*) trajectories of vortices of unstable quadrupolar roundabouts.

ideas of investigation of the invariant sets of stability in dynamic systems having several first integrals were used. Routh, Lyapunov, Levi-Civita, and many others worked in this field (see [14]). Kizner [11] used the following definition: the vortex multipole is steady if, at a reasonably small initial perturbation of distances between its vortices, these distances remain weakly perturbed for all time. Such stability does not exclude that with time, the multipole goes away from the unperturbed position to an arbitrary large distance. Therefore, the stability by Routh (see Fig. 4*a*) does not follow from it. The most complete results in [11] were obtained for $N = 2$ (the stability was proved in the exact nonlinear formulation for all values of parameters from white and dark regions in Fig. 1*a*), and for the cases of $N = 3$, 4, restrictions were imposed on the intensities of vortices and on perturbations of the initial data.

Homogeneous ideal fluid. It is the case II at $\alpha = 1$, i.e., at $V(\xi) = W(\xi) = \ln\xi$. The vortex tripole is exponentially unstable at $\Gamma > -\frac{5}{4}$ and linearly stable at $\Gamma < -\frac{5}{4}$ (a nonlinear analysis is required). The vortex quadrupole is exponentially unstable when $\Gamma > 1$, linearly stable at $\Gamma < 0$ (a nonlinear analysis is required), and stable by Routh if $0 < \Gamma < 1$.

Remark 2. As to the stability in the problem of $N + 1$ vortices in the Kirchhoff model (homogeneous fluid), one usually refers to [15]. In this study, it is wrongly affirmed that the vortex tripole (quadrupole) is stable by Lyapunov at $-\frac{1}{4} < \Gamma < \frac{1}{4}$ $\left(-\frac{1}{2} < \Gamma < 1\right)$ and exponentially unstable under rough violation of this condition. The correct condition of the exponential instability is specified in [9].

ACKNOWLEDGMENTS

The work of the first author was supported by the Ministry of the Russian Federation (project no. 1.1398.2014/K), and the work of the third author was supported by Russian Science Foundation (project no. 14-50-00095)

REFERENCES

1. P. K. Newton, *The N-Vortex Problem: Analytical Techniques. Ser. Appl. Math. Sci.* (N.Y.; B.; Heidelberg: Springer, N.Y., 2001), Vol. 145.

2. M. A. Sokolovskiy and J. Verron, *Dynamics of Vortex Structures in a Stratified Rotating Fluid. Ser. Atmospheric and Oceanographic Sciences Library* (Cham; Heidelberg; N.Y.; Dordrecht; L.: Springer, 2014), Vol. 47.
3. L. G. Kurakin and V. I. Yudovich, The Stability of Stationary Rotation of a Regular Vortex Polygon, Chaos **12** (3), 574 (2002).
4. L. G. Kurakin, On the Nonlinear Stability of Regular Vortex Polygons and Polyhedrons on a Sphere, Dokl. Phys. **48** (2), 84 (2003).
5. L. G. Kurakin, Stability, Resonances, and Instability of Regular Vortex Polygons in a Circular Domain, Dokl. Phys. **49** (11), 658 (2004).
6. L. G. Kurakin and I. V. Ostrovskaya, Nonlinear Stability Analysis of a Regular Vortex Pentagon Outside a Circle, Reg. Chaot. Dyn. **17** (5), 385 (2012).
7. L. G. Kurakin, Influence of Annular Boundaries of Thomson's Vortex Polygon Stability, Chaos **14**, 023105 (2014).
8. L. G. Campbell, Influence of Annular Boundaries of Thomson's Vortex Polygon Stability, Phys. Rev. A **24** (1), 514 (1981).
9. G. K. Morikawa and E. V. Swenson, Interacting Motion of Rectilinear Geostrophic Vortices, Phys. Fluids **14** (6), 1058 (1971).
10. M. A. Sokolovskiy and J. Verron, *Motion of A + 1 Vortices in a Two-Layer Rotating Fluid,* in *IUTAM Symp. on Hamiltonian Dynamics, Vortex Structures, Turbulence. IUTAM Bookseries* (Springer, Heidelberg, 2008), Vol. 6, p. 481.
11. Z. Kizner, On the Stability of Two Layer Geostrophic Point Vortex Multipoles, Phys. Fluids **26**, 046602 (2014).
12. V. M. Gryanik, Dynamics of Singular Geostrophic Vortices in a Two-Level Model of Atmosphere (Ocean), Izv. AN SSSR. FAO **19** (3), 227 (1983).
13. V. I. Arnol'd, *Mathematical Methods of Classical Mechanics* (Editorial URSS, Moscow, 2003) [in Russian].
14. A. V. Karapetyan, *Stability of Steady Motions* (Editorial URSS, Moscow, 1998) [in Russian].
15. H. E. Cabral and D. S. Schmidt, Stability of Relative Equilibria in the Problem on N + 1 Vortices, SIAM J. Math. Anal. **31** (2), 231 (1999).

Translated by V. Bukhanov